

Spatial and temporal distribution of the invasive *Gracilaria vermiculophylla* through remote sensing at its first described European site

Simon Oiry¹ Bede Ffinian Rowe Davies¹ Pierre Gernez¹
Laurent Barillé¹

2024-12-17

To be Written

¹

1 Title proposition

- Remote Sensing of *Gracilaria vermiculophylla* in the site of its First European Observation
- Monitoring the marine invasive alien species *Gracilaria vermiculophylla* using unmanned aerial vehicles
- Remote Sensing of *Gracilaria vermiculophylla*: Mapping its Distribution at the Site of its First European Description
- Mapping the Spread of the Invasive Species *Gracilaria vermiculophylla* using Remote Sensing at the Site of its Initial Description in Europe
- Quantifying *Gracilaria vermiculophylla* Spatial and Temporal Distribution Through Remote Sensing at its First Recorded European Site

¹Institut des Substances et Organismes de la Mer, ISOMer, Nantes Université, UR 2160, F-44000 Nantes, France

2 Introduction

The introduction of Non-Indigenous Species (NIS) in terrestrial, freshwater, and marine ecosystems is one of the major threats to biodiversity worldwide. In particular, the proliferation and rapid spread of Invasive Alien Species (IAS) can radically change the structure and functioning of marine ecosystems, , requiring effective inventorying and monitoring programs (Massé et al., 2023). In Europe, 874 NIS have been introduced to the marine environment so far (i.e. until 2020) and it is expected that the rate of biological invasions will continue to increase in the coming years (Zenetos et al., 2022). Macroalgae represent more than 40 % of the NIS introduced to Europe waters, with many species native to the Temperate Northern Pacific (Williams and Smith, 2007). Amongst all invasive macroalgae, *Gracilaria vermiculophylla* (Papenfuss, 1967) (original name *Gracilaria vermiculophylla* (OHMI, 1956); also known as *Agarophyton vermiculophyllum* (Gurgel et al., 2018)), has spread extensively from its native distribution range in Japan and Korea (Terada and Yamamoto, 2002) across temperate estuaries in North America, Europe, and other regions, facilitated by aquaculture and maritime activities (Krueger-Hadfield et al., 2017; Rueness, 2005; Weinberger et al., 2008). While *G. vermiculophylla* can provide some ecosystem services, such as habitat for invertebrates and juvenile fish (Davoult et al., 2017), it often outcompetes native vegetation, alters sediment composition (Nyberg et al., 2009), and disrupts trophic interactions (Ginneken et al., 2018). In regions like the Baltic Sea and the eastern United States, it has been documented to negatively affect native fucoids and seagrasses (Firth et al., 2024; Thomsen et al., 2013; Van Katwijk, 2003). These impacts underscore the importance of monitoring and managing the spread of *G. vermiculophylla*, particularly as climate change and anthropogenic pressures continue to facilitate biological invasions. *G. vermiculophylla* success as an invader stems from its tolerance to a wide range of environmental conditions, including temperature (Sotka et al., 2018), nutrient variability (Abreu et al., 2011) and salinity (Weinberger et al., 2008). Its growth capacity at low salinities (Nyberg, 2007; Rueness, 2005) explains its presence in the brackish waters of the Baltic Sea (Weinberger et al., 2008) but also in the mesohaline sheltered part of estuaries of the Atlantic coast of Europe (**Surget et al., 2017**). It is also present in confined areas of lagoons characterized by low hydrodynamism (Abreu et al., 2011; Sfriso et al., 2012). In Europe, it was first observed in 1996 in the Belon estuary (France) and later in many other estuaries on the Brittany coast of France (Rueness, 2005). It can be found on hard substrates such as invertebrate's tubes and shells providing a substratum (Thomsen et al., 2007) or attached to pebbles and rocks (Terada and Yamamoto, 2002) but the largest populations are colonizing soft-bottom sediment and particularly estuarine intertidal mudflats (**Surget et al., 2017**). In this habitat, extensive dark red mats are observed at low tide, covering vast areas that have largely been unquantified in most studies. Therefore, *G. vermiculophylla* is capable of establishing populations in soft-bottom sediment habitats that were previously devoid of macroalgae (Ramus et al., 2017). These mats are usually monospecific with the alga thalli partially buried into the mud (Rueness, 2005; Surget, 2017). Intertidal mats can however be temporarily overgrown by ephemeral green macroalgae (Weinberger et al., 2008). In the estuaries where *G. vermiculophylla* was first documented, large monospecific

mats were reported to be confined to the upper intertidal zones (Rueness, 2005); however, their spatial distribution relative to the mudflat topography had not been quantitatively assessed. In fact, *G. vermiculophylla* has never been mapped using remote sensing techniques, and existing descriptions of its distribution lack spatially explicit mapping (Abreu et al., 2011; Sfriso et al., 2012; Thomsen et al., 2007; Weinberger et al., 2008)

Remote sensing has revolutionized our ability to monitor and manage coastal ecosystems, offering efficient and scalable methods for detecting environmental changes in intertidal vegetation across a wide range of spatio-temporal scales (Calleja et al., 2017; Davies et al., 2024a, 2024b; Valle et al., 2015; Zoffoli et al., 2021). Among remote-sensing technologies, drone-based imagery has recently emerged as a particularly promising tool for studying the spatial distribution of intertidal primary producers such as benthic microalgae (Román et al., 2024, 2021), seagrass (Chand and Bolland, 2021; Duffy et al., 2018; Román et al., 2021) and macroalgae (Diruit et al., 2022; Peidro-Devesa et al., 2024). While it lacks the temporal consistency of satellite missions, drone remote sensing makes it possible to acquire at extremely high spatial resolution (i.e. cm-scale), rapidly target specific areas of interest, and to provide observations in overcast conditions. In particular, the potential of drone remote sensing for monitoring the surface area occupied by IAS has been demonstrated (Roca et al., 2022). Drone-based photogrammetry also makes it possible to characterize the distribution of intertidal vegetation together with mudflat geomorphology, thus improving our understanding of primary producers patterning (Brunier et al., 2022; Douglas et al., 2024).

In this study, a drone-based multispectral remote sensing approach was applied to map *G. vermiculophylla* spatial distribution at a very-high spatial resolution in three intertidal estuaries of European Atlantic coast. We adapted the neural network classification model DISCOV (Drone Intertidal Substrate Classification Of Vegetation, Oiry et al. (2024b), Oiry et al. (2024a)) by specifically training the model with a new class corresponding to *G. vermiculophylla*. A validation dataset was obtained from *in situ* data to estimate the classification accuracy. LiDAR data were concurrently acquired to accurately map the intertidal elevation. We used a Generalized Additive Model (GAM) to examine the relationship between the seaweed spatial distribution and spatial metrics quantifying the mudflat topography. We expected the presence of *G. vermiculophylla* in mudflats to be associated to a specific height range as well as being more closely related to flat areas of the intertidal zone.

3 Materiel & Methods

3.1 Study sites

Field campaigns were conducted at three study sites in France and Spain. At each site, two locations were investigated Figure 1. The Aven & Belon Estuary in South Brittany, France (Figure 1 A & C), is a dynamic ria-type system hosting diverse habitats, including sandy tidal flats and subtidal zones with coarse, marine-origin sediments (Castaing and Guilcher, 1995;

Michel et al., 2021). These habitats support key benthic species such as *Scrobicularia plana*, *Cerastoderma edule*, and *Tellina tenuis*, which play essential roles in sediment bioturbation and nutrient cycling (Blanchet et al., 2014; Tankoua et al., 2011). The estuary serves as a nursery for juvenile fish and a feeding ground for migratory birds, with its ecological productivity driven by a mix of euryhaline and marine species adapted to salinity gradients (Blanchet et al., 2014). Oyster farming, particularly *Crassostrea gigas*, is a dominant activity, altering sediment dynamics and local biodiversity (Michel et al., 2021). Despite its ecological richness, the estuary faces pressures from nutrient loading and physical alterations, with bioindicators like *S. plana* used to monitor the impacts of salinity, sediment quality, and pollution (Tankoua et al., 2011).

The Saja-Besaya Estuary, situated along the Cantabrian Sea in northern Spain, is characterized by the confluence of the Saja and Besaya rivers near Torrelavega (Figure 1 C). The estuary, also known as San Martín de la Arena or Suances Estuary, has been subject to significant anthropogenic pressures, including industrial developments throughout the 20th century. These activities have led to contamination from mining, paper manufacturing, and carbonate discharges, classifying the estuary as highly polluted near its upper reaches (Ortega et al., 2005). This contamination impacts the estuarine ecosystem, including water quality and biodiversity, with minimal aquatic life and sparse riverbank vegetation in its lower sections (Romero et al., 2008).

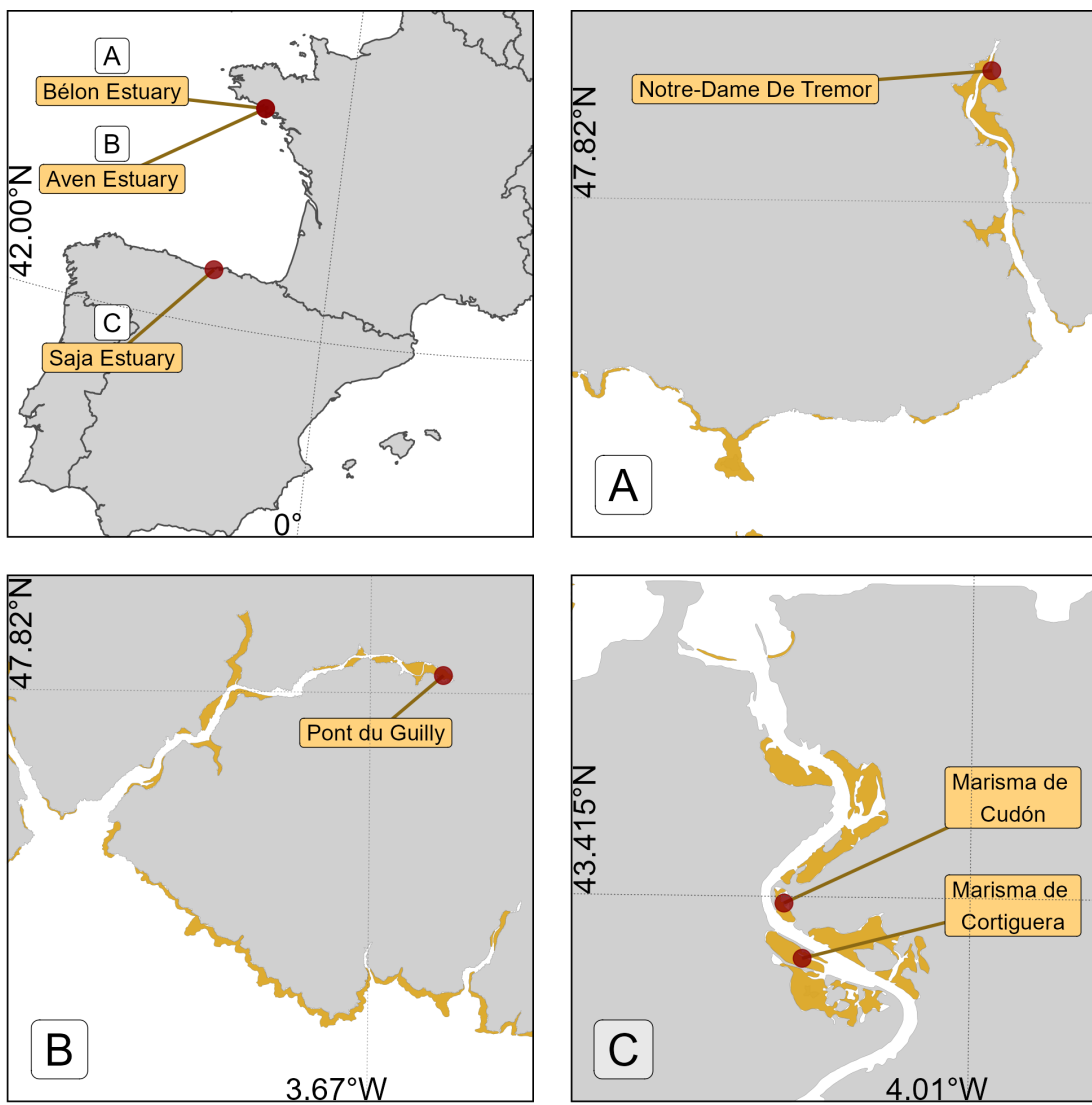


Figure 1: Location of the drone flights. A: Flights made in Aven Estuary, France; B: Flights made in Bélon Estuary, France; C: Flights made in Saja Estuaries, Spain. Golden polygons represent intertidal areas.

3.2 Remote sensing data acquisition and pre-processing

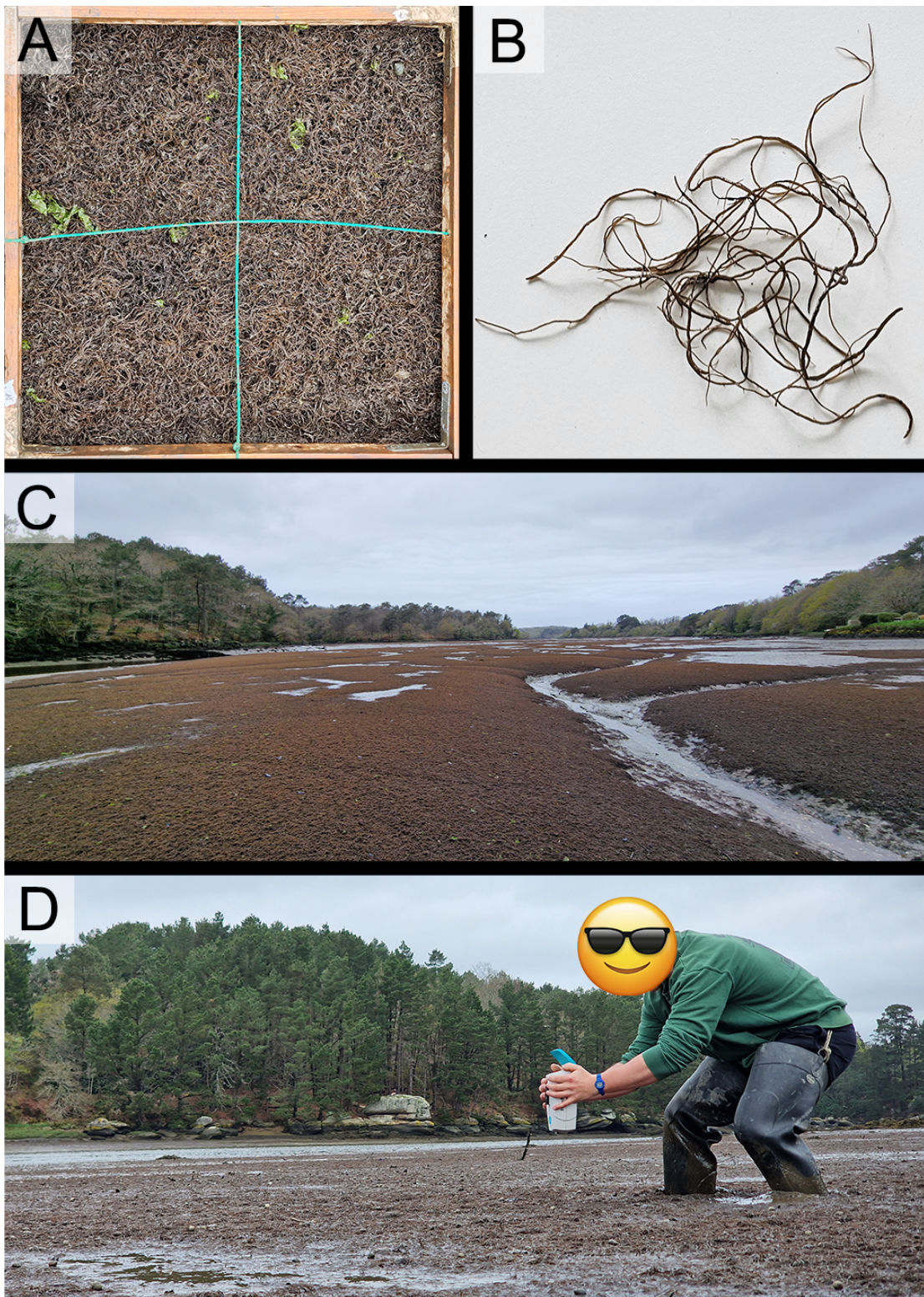


Figure 2: Pictures of *Gracilaria vermiculophylla*. A: Quadrat of 0.25 m² with a high cover of *G. vermiculophylla*; B: Single thallus of the algae; C: Landscape view with a high coverage of *G. vermiculophylla*; D: Recording of the spectral signature of the algae using an ASD FieldSpec HandHeld 2 spectroradiometer.

3.2.1 Hyperspectral measurements

At each location, hyperspectral reflectance signatures were recorded using an ASD FieldSpec HandHeld 2 spectroradiometer (Malvern Panalytical, Worcestershire, UK), which measures reflectance from 325 to 1075 nm with a spectral resolution of approximately 1 nm Figure 2. Each spectrum was subsequently smoothed using a Savitzky–Golay filter (Savitzky and Golay, 1964) with a third-order polynomial and an 11-point window, selected to minimize noise while preserving salient spectral features. After this initial smoothing, the first and second derivatives were computed using a central difference approximation (Equation 1).

$$f''(\lambda_i) \approx \frac{f(\lambda_{i+1}) - 2f(\lambda_i) + f(\lambda_{i-1})}{(\Delta\lambda)^2} \quad (1)$$

where $f(\lambda_i)$ is the reflectance at wavelength λ_i and $\Delta\lambda$ is the uniform spectral sampling interval.

3.2.2 Drone data

Table 1: List of drone flights, summarising the location, the date, and the total extent of each flight (in hectars).

| Country | Site | Flight | Date | Area |
|---------|--------------|-----------------------|------------|------|
| France | Aven & Belon | Notre-Dame De Tremor | 2024-04-11 | 26.7 |
| | | Pont du Guilly | 2024-04-11 | 21.3 |
| Spain | Saja Estuary | Marisma de Cortiguera | 2024-06-25 | 20.4 |
| | | Marisma de Cudón | 2024-06-25 | 8.4 |

A total of 6 drone flights were done spread in the 3 study sites. Each time, flights were done at an altitude of 120 m and at a speed of 10 m.s⁻¹ (Table 1).

3.2.2.1 Multispectral data

At each location, reflectance images with a resolution of 1.2 million pixels were captured using a DJI Matrice 300 quadcopter drone equipped with a Micasense RedEdge Dual MX multispectral camera. The camera recorded data across ten spectral bands, spanning from blue to near-infrared (NIR) wavelengths (444, 475, 531, 560, 650, 668, 705, 717, 740, and 840 nm) (). To ensure consistent lighting conditions, the drone's flight trajectory was aligned to maintain a solar azimuth angle of 90 degrees. Image acquisition was carried out with an overlap of

70% between side-by-side images and 80% between successive images along the flight path. A downwelling light sensor (DLS2) was used to measure real-time irradiance, enabling the correction of reflectance values for variations in light intensity caused by cloud cover during the flight. The raw image data were subsequently calibrated to reflectance using a calibration panel with ~50% reflectivity, provided by the camera's manufacturer. Images were processed using structure-from-motion photogrammetry software (Agisoft, 2019) to generate multispectral ortho-mosaics for each flight. The ortho-mosaicking workflow was consistent across all flights. Initially, key tie points were identified within each image and across overlapping images to create a sparse point cloud. This point cloud was refined by removing noisy points using a reprojection accuracy metric. Subsequently, a dense point cloud was generated using a structure-from-motion algorithm. A digital surface model (DSM) was then created through surface interpolation of the dense point cloud, which served as the basis for reconstructing the multispectral ortho-image (Nebel et al., 2020). The resolution of the multispectral ortho-mosaic obtained were 8 cm per pixel.

3.2.2.2 LiDAR data

LiDAR standing for Light Detection and Ranging uses lasers to measure distances by timing reflected pulses, creating detailed 3D maps of surfaces.

Using the Matrice 300 Series Dual Gimbal Connector, a DJI Zenmuse L1 LiDAR and RGB sensor was mounted on the drone alongside a multispectral camera. This setup enabled the simultaneous capture of LiDAR point clouds, high-resolution RGB images, and multispectral images collected by the MicaSense RedEdge Dual MX during the same flight. The same processing workflow as Section 3.2.2.1 was applied to process LiDAR RGB images, resulting in ortho-mosaic with a resolution of 2.5 cm per pixel. Since the mapping focused solely on flat surfaces without dense vegetation, the LiDAR measured only a single return. Operating in repetitive scanning mode with a sampling rate of 240 kHz, the system achieved a point density of 350 points per square meter. The LiDAR point cloud was extracted and converted into LAS format using DJI Terra software. The LAS point cloud was then imported into Agisoft Metashape (Agisoft, 2019) to generate a Digital Surface Model (DSM) with a resolution of 2.5 cm. From the DSM, the slope of each pixel based on a grid of 8 surrounding pixels were computed using the terrain function of the 'terra' package in R (Hijmans, 2024). The angle of the mudflat was categorized into three classes: Flat (angle < 10°), Angled (10° < angle < 40°), and Vertical (angle > 40°).

3.3 Scene classification

A neural network classification model (DISCOV; Oiry et al. (2024b); Oiry et al. (2024a)), previously applied with success to Micasense reflectance data for mapping intertidal vegetation along the Portuguese and French Atlantic coasts, has been used in this study. The training dataset of DISCOV v1.0 has been updated. As shown by Oiry et al. (2024b) the DISCOV

v1.0 model (Oiry et al., 2024a) was trained using only 5771 Rhodophyceae pixel (3% of the training dataset). To fill this gap the original training dataset of DISCOV v1.0 was updated using new training pixel coming from the 5 drone flights (Section 3.2). A total of 427000 pixels were added to the DISCOV training dataset compared to the version 1 (Table 2).

Table 2: Class of the Neural Network model, with the number of training pixels used to train that class and the differences with the training dataset of DISCOV v1.0

| Name | Taxonomic Class | Training Pixels | Difference with DISCOV v1.0 |
|------------------|-------------------|-----------------|-----------------------------|
| Benthic Diatoms | Bacillariophyceae | 62,436 | x13.95 |
| Green macroalgae | Chlorophyta | 92,585 | x5.4 |
| Seagrass | Magnoliopsida | 221,065 | - |
| Brown macroalgae | Phaeophyta | 169,936 | - |
| Red macroalgae | Rhodophyta | 268,637 | x46.55 |
| Sediment | - | 117,956 | x1.24 |
| Water | - | 91,614 | x1.09 |

To validate the new version of the DISCOV model, a Shiny app was developed, enabling independent users to photo-interpret snapshots of the ortho-mosaic from each drone flight (Chang et al., 2024; Simon, 2024). Users could click on various parts of the snapshots to indicate the type of vegetation they believed was present. Using this method, 3 independent users contributed to creating a validation dataset of 6755 pixels across 79 snapshots distributed among the four drone flights Table 3. The validation dataset was then simplified into two classes: Presence or Absence of Red Algae.

Table 3: Presence and absence of red macroalgae for each drone flight

| Site | Absent | Present | Total |
|-----------------------|--------|---------|-------|
| Marisma de Cortiguera | 1,531 | 483 | 2,014 |
| Marisma de Cudón | 1,237 | 136 | 1,373 |
| Notre-Dame De Tremor | 1,073 | 463 | 1,536 |
| Pont de Guilly | 1,389 | 443 | 1,832 |
| Total | 5,230 | 1,525 | 6,755 |

3.4 Historical Presence of *Gracilaria vermiculophylla* in the Bélon estuary

To assess the historical presence of *G. vermiculophylla* in the Bélon Estuary, aerial imagery from flight campaigns was obtained via the IGN platform “Remonter Le Temps” (IGN, 2024). Nine images were selected between 1952 and 2012 from the IGN plateform and an additional one has been added for the year 2024 (Table 4). Since most of the images retrieved from “Remonter Le Temps” were digitized versions of physical photographs, georeferencing were required.

Table 4: Images used to assess the historical presence of *Gracilaria vermiculophylla* in the Belon esturay. Images from the IGN data source have been retrieved from the “Remonter Le Temps” plateform (IGN, 2024). Drone flight have been performed by the team using a Mavic 3 Entreprise.

| Date | Type | Data Source | Resolution (cm per Pixel) |
|------------|-----------------|--------------|---------------------------|
| 1952-04-26 | Black and White | IGN | 10 |
| 1958-04-22 | Black and White | IGN | 90 |
| 1976-07-? | Black and White | IGN | 4 |
| 1978-08-22 | Black and White | IGN | 44 |
| 1982-08-11 | Black and White | IGN | 44 |
| 1992-05-17 | True Color | IGN | 70 |
| 1997-04-11 | Black and White | IGN | 64 |
| 2012-07-24 | True Color | IGN | 18 |
| 2024-04-11 | True Color | Drone Flight | 3 |

For each date, polygons have been drawn around *G. vermiculophylla* patches by visually photo-interpreting on each images. These polygons were used to calculate the total area of the mudflat covered by macroalgae within a common extent of 30 hectares in Pont de Guilly, located in the Bélon Estuary, South Brittany, France.

4 Results

4.1 Historical records in the Belon estuary

A clear shift in sediment coloration over the paste 70 years were observed, closely aligned with the subsequent proliferation of the invasive red macroalga *Gracilaria vermiculophylla*

(Figure 3). Before 1976, the sediments appeared relatively light, indicating no detectable presence of this species. Following its initial appearance in 1976, subtle darkening of the sediment became discernible, coinciding with the early establishment of *G. vermiculophylla*. During the subsequent decades, the late 1970s through the 1990s, this darkening trend became more pronounced and widespread, reflecting an increasing spatial coverage and biomass of the algae. By the early 2000s, and especially by 2024, the sediment exhibited consistently darker tones, indicative of extensive and persistent colonization by *G. vermiculophylla*.

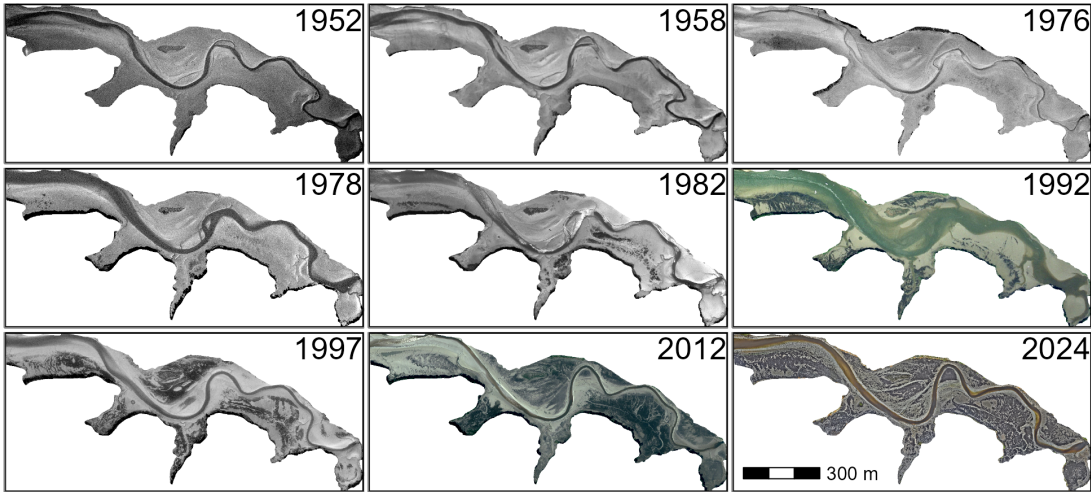


Figure 3: Historical images of Pont du Guilly between 1952 and 2024.

From the early recordings in the 1950s through the late 1970s, *Gracilaria vermiculophylla* coverage remained effectively at 0% (Figure 4). Shortly after the introduction of *Crassostrea gigas* in the estuary (see vertical red dashed line in the figure), the first detectable presence of *G. vermiculophylla* emerged. By 1976, it covered 2.5% (0.7 ha) of the Pont du Guilly area, and by 1978 it had increased slightly to 3.0% (0.9 ha). From 1982 onward, coverage expanded more rapidly, increasing from 6.6% (2.0 ha) in 1982 to 14.7% (4.5 ha) in 1992 and nearly 30% (9.0 ha) by 1997. This upward trend continued into the 21st century, peaking at 43.8% (13.3 ha) in 2012. Although coverage fluctuated somewhat thereafter (40.6% in 2019 and 40.2% in 2024), it remained consistently high, indicating sustained and widespread colonization.

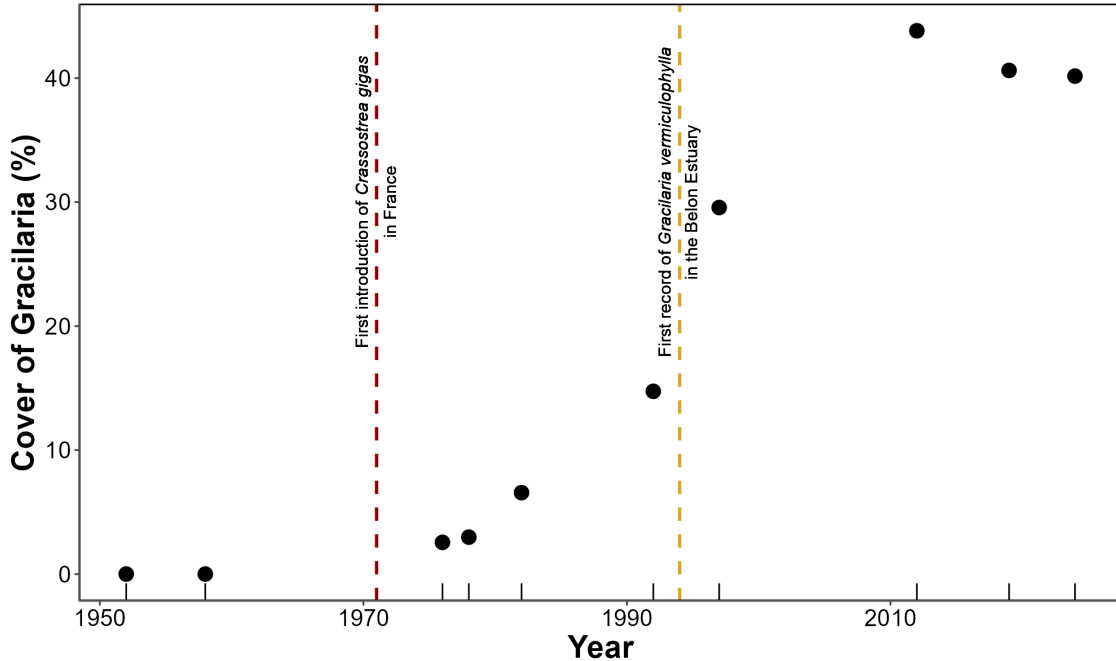


Figure 4: Evolution of the *Gracilaria vermiculophylla* cover at Pont du Guilly in the Belon Estuary. The red vertical line indicates the date of *Crassostrea gigas* introduction in France (Grizel and Heral, 1991), while the golden line represents the date of the first documented mention of *Gracilaria vermiculophylla* invasion in France in the literature (Rueness, 2005).

4.2 Spectral description

The spectral signature of *Gracilaria vermiculophylla* was characterized by a wavy reflectance pattern in the visible region of the spectrum, between 500 and 700 nm (Figure 5 A). This pattern was primarily driven by the presence of phycoerythrin and phycocyanin, which exhibited maximum absorption peaks at approximately 565 nm and 620 nm, respectively. An additional absorption feature around 495 nm was likely attributable to the presence of accessory carotenoid pigments. The most pronounced absorption peak occurred at 675 nm, corresponding to chlorophyll-a absorption. The second derivative analysis clearly highlighted the inflection points corresponding to the main absorption peaks at 495, 565, 620, and 675 nm, allowing for a more precise identification of the spectral contributions of these pigments (Figure 5 B).

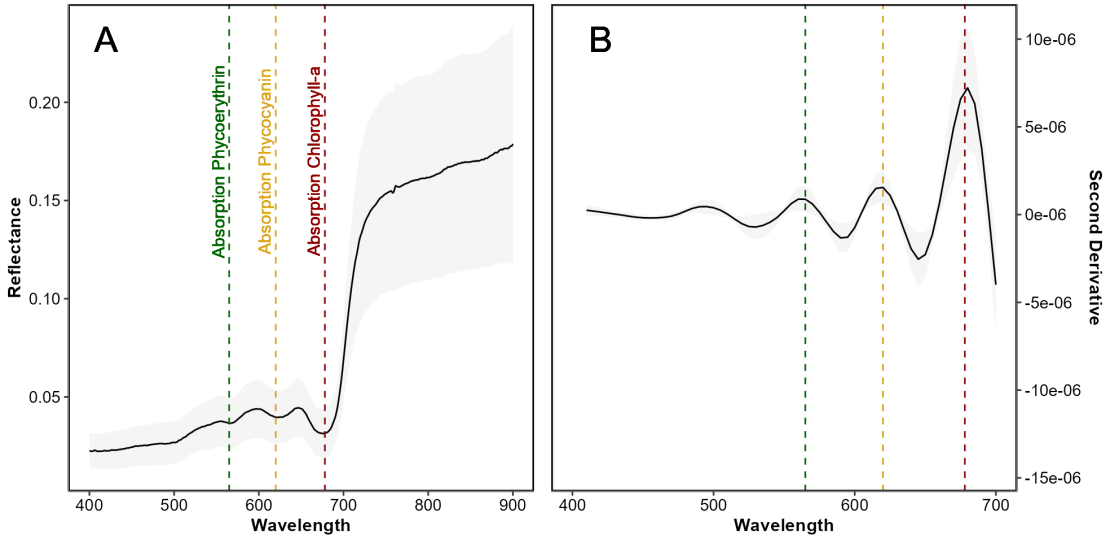


Figure 5: Hyperspectral signature of *Gracilaria vermiculophylla* (A) and its second derivative (B). The black line represents the average spectra, while the shaded ribbon indicates the standard deviation. Dashed lines mark the absorption maxima of Phycoerythrin, Phycocyanin, and Chlorophyll-a, shown in green, orange, and red, respectively.

4.3 Spatial distribution

The classification map illustrates the diversity of benthic communities and substrates in the study area (Figure 6 A and B). Rhodophyceae (red) emerges as the dominant algal cover, forming extensive, continuous patches aligned with the mid-intertidal zones. In contrast, Bacillariophyceae (orange) and Chlorophyceae (green) exhibit more localized distributions, typically restricted to smaller, fragmented patches where specific microtopographic or hydrodynamic conditions favor their presence. Phaeophyceae (brown) is confined to limited patches, often found near transitional zones between sediment and water or in the upper intertidal area, where it is attached to rocky substrates. The water class (blue) delineates the main tidal channel, which meanders through the center of the area and influences the distribution of adjacent habitats. Across the for study sites the presence/absence of *G. vermiculophylla* were classified with a global accuracy of 91.1 %, a sensitivity of 96.5 % and a specificity of 71.5 %.

The bathymetric map reveals a continuous gradient in elevation relative to mean sea level (Figure 6 C). A comparison of bathymetry and vegetation distribution highlights a clear elevation-driven pattern in algal presence. Higher intertidal zones, located above the deeper channel areas, are associated with more extensive algal communities. In contrast, lower intertidal zones closer to the channel consistently exhibit reduced macroalgal cover.

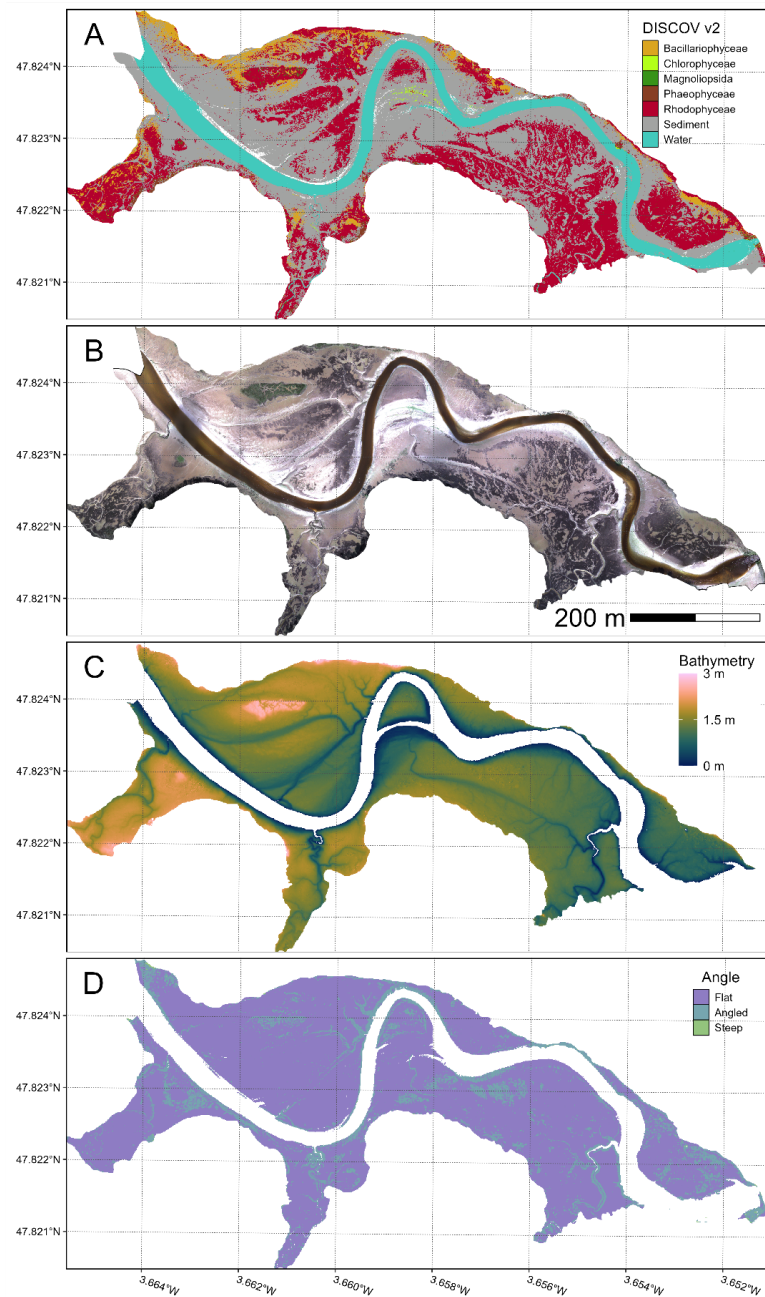


Figure 6: DISCOV Prediction (A), RGB composition (B), Bathymetry (C) and mudflat angle (D) of the Bélon estuary site in Brittany, France. The total extent of this flight was 21 hectares with a resolution of 8 mm per pixel. Bathymetry is represented as the height above mean sea level.

Overall, the percent cover of *Gracilaria vermiculophylla* increases with bathymetry, as shown by the general relationship (Figure 7, black line), which rises from approximately 16% at the lowest elevation to about 30% at the highest elevation. This indicates a consistent positive association between bathymetry and algal cover.

When accounting for slope, the flatter the slope, the higher the percent cover of *G. vermiculophylla*. For flat slopes, the cover ranges from approximately 20% at the lowest elevation to nearly 38% at the highest elevation. In contrast, for angled slopes, the increase is less pronounced, ranging from around 16% to 32%. On steep slopes, the cover is the lowest, starting at about 15% and rising only slightly above 30% at the highest elevation (Figure 7). This demonstrates that slope modifies the relationship, with flatter slopes supporting a greater percent cover of the algae.

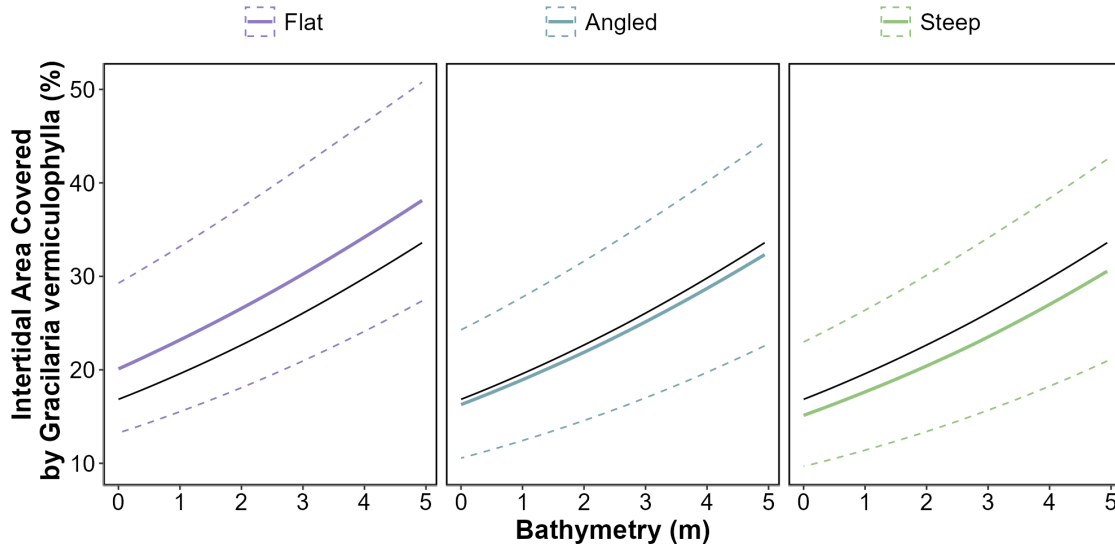


Figure 7: DISCOV Prediction (A), RGB composition (B) and Bathymetry (C) of the Bélon estuary site in Brittany, France. The total extent of this flight was 21 hectares with a resolution of 8 mm per pixel. Bathymetry is represented as the height above mean sea level.

5 Discussion

5.1 Drone mapping *G. vermiculophylla* with machine learning

In this study, we produced the first spatial distribution maps of the invasive red alga *Gracilaria vermiculophylla* using a multispectral drone survey conducted at low tide in Atlantic estuaries representing varied environmental conditions. In southern Brittany, the species formed

monospecific mats, while in the Cantabrian region of Spain, it was intermixed with other intertidal vegetation. Distinguishing among these vegetation types was a key prerequisite for the analysis.

To achieve this, we adapted the deep learning-based classification model DISCOV (Oiry et al., 2024b), initially developed to discriminate seagrass from green macroalgae. Although the original model included Rhodophyceae as a class, this group constituted less than 3% of its training dataset. In contrast, the updated model presented here was trained on a dataset in which *G. vermiculophylla* covered 26 % of approximately one million pixels. This improved dataset allowed the model to achieve an accuracy of 91.1 %.

Rhodophytes possess unique phycobilin pigments, enabling their spectral distinction from other macroalgal groups (Douay et al., 2022; Mcilwaine et al., 2019; Olmedo-Masat et al., 2020). Even with the ten-band multispectral sensor used in our study, it remained feasible to discriminate the major classes of intertidal macrophytes (Davies et al., 2023; Oiry et al., 2024b; Román et al., 2021). However, the model identifies *G. vermiculophylla* at the class level (Rhodophyceae) rather than at the species level. Although hyperspectral approaches may allow finer taxonomic resolution (Douay et al., 2022; Olmedo-Masat et al., 2020), it is unlikely that *Gracilaria* species can be precisely distinguished using standard multispectral sensors.

Ecological factors also aid in differentiating *G. vermiculophylla*. Unlike many other macroalgae that require hard substrates, *G. vermiculophylla* establishes itself on soft-bottom sediments. In fact, it is commonly found on mudflats, anchoring its thalli in the top 10 cm of mud (Surget, 2017), and inhabits the upper intertidal zone—an unusual trait for a Rhodophyte (Abreu et al., 2011; Davoult et al., 2017). By reliably detecting *G. vermiculophylla* in these soft-substrate, upper intertidal habitats, our method provides a framework for identifying environmental conditions that favor its spread, potentially offering managers early-warning indicators to control its expansion before it reaches nuisance levels. Thus, combining spectral data with sediment characteristics provides a strong indicator of *G. vermiculophylla* presence in European Atlantic estuaries, complementing the physical variables already used in species distribution modeling (Mendoza-Segura et al., 2023).

In addition, the scalability of drone-based surveying facilitates repeat mapping to detect temporal shifts in the distribution and abundance of *G. vermiculophylla*. Such continuous monitoring could capture seasonal patterns of colonization, allowing researchers and environmental managers to evaluate the effectiveness of mitigation measures, track long-term ecological impacts, and anticipate future shifts in habitat suitability under changing climate conditions.

5.2 *G. vermiculophylla* spatial distribution and mudflat topography

The spatial distribution of *Gracilaria vermiculophylla* across intertidal zones reveals a distinct relationship with mudflat topography, which significantly influences algal density and coverage. Our results show that higher elevations within the intertidal zone support greater densities of *G.*

vermiculophylla, a pattern that aligns with findings by Thomsen et al. (2009), where elevated areas provided optimal conditions for algal survival. Conversely, areas with steeper slopes exhibited lower algal abundance. This inverse relationship between slope and algal density may be attributed to increased erosion or less stable sediment conditions, which inhibit the algae's ability to anchor and accumulate (Besterman et al., 2021)

5.3 Spatio-temporal monitoring of invasive macroalgae

Accurate, high-resolution maps of invasive or alien species are extremely scarce (Fourcade et al., 2014; Vilizzi et al., 2021), yet they enable in-depth evaluations of these species' ecology, temporal dynamics, and niche behavior in relation to their environment. In this study, using individual flights over monospecific algal mats, we quantified how this invasive alga associates with local mudflat topography, demonstrating that its distribution is closely tied to specific topographical features, such as elevation and slope gradients. This relationship reveals how physical features of the mudflat can influence the extent and density of *Gracilaria vermiculophylla* mats. Understanding the drivers of the spatial distribution of the algae helps to anticipate the future development of this species and identify areas vulnerable to its invasion. Repeated monitoring of this type can further reveal phenological patterns, invasion dynamics, and local conspecific biological interactions—such as co-occurrence, displacement, or avoidance (Arim et al., 2006; Godoy et al., 2009).

Remote sensing using multispectral drone mapping can provide high-resolution, spatially explicit data, but it must be combined with repeated, in situ field measurements to maximize its potential (Chadwick et al., 2020; Zoffoli et al., 2023). As noted, temporal repetition makes it possible to assess dynamic processes, and integrating these mapping approaches with in situ analyses of local infauna, carbon cycling, riverine inputs, and sedimentology would yield valuable insights for local managers. Such an integrated approach could help determine how the invasive algae affects the local ecosystem and, more broadly, forecast its potential impact on other estuarine environments facing similar invasion events. This holistic approach can guide strategic interventions aimed at mitigating the alga's spread, maintaining ecological balance, and protecting native biodiversity, ensuring that management efforts are informed by accurate, timely, and spatially explicit data.

Invasive species like *Gracilaria vermiculophylla* and *Rugulopteryx okamurae* can be identified using drones equipped with multispectral sensors, taking advantage of the characteristic reflectance of rhodophytes (Barillé et al., 2025; Nurdin et al., 2023). However, while RGB sensors on readily available commercial drones can be used to perform accurate scene classification, their effectiveness for mapping invasive species has not yet been demonstrated (Cheng et al., 2017; Kazakeviciute-Januskeviciene et al., 2020). These drones are easy to deploy, can cover large areas when flying at speeds of 15 m s^{-1} at an altitude of 120 m, and still maintain sufficient overlap between images to support photogrammetric reconstruction. Expanding these methodologies to RGB-based detection would significantly lower barriers to entry, allowing local stakeholders with limited resources to access valuable monitoring tools for early detection

and rapid response. A promising avenue for operational applications lies in testing machine learning techniques for coastal habitat mapping using RGB imagery that do not rely on enhanced spectral resolution. Considering the low cost of RGB and multispectral commercial drones, coupled with ongoing advancements in machine learning, drone-based remote sensing has now matured into a practical tool for adoption by environmental authorities in coastal management. Integrating these technologies into routine monitoring protocols can enhance surveillance capabilities, improve understanding of invasive species dynamics, and ultimately contribute to more effective conservation and restoration strategies.

6 Conclusion

References

- Abreu, M.H., Pereira, R., Buschmann, A., Sousa-Pinto, I., Yarish, C., 2011. Nitrogen uptake responses of *gracilaria vermiculophylla* (ohmi) papenfuss under combined and single addition of nitrate and ammonium. *Journal of Experimental Marine Biology and Ecology* 407, 190–199.
- Agisoft, 2019. [Agisoft metashape](#).
- Arim, M., Abades, S.R., Neill, P.E., Lima, M., Marquet, P.A., 2006. Spread dynamics of invasive species. *Proceedings of the National Academy of Sciences* 103, 374–378.
- Barillé, L., Paterson, I.L., Oiry, S., Aris, A., Cook-Cottier, E.J., Nurdin, N., 2025. Variability of *kappaphycus alvarezii* cultivation in south-sulawesi (indonesia) related to the monsoon shift: Water quality, growth and colour quantification. *Aquaculture Reports* 40, 102557.
- Besterman, A.F., McGlathery, K.J., Reidenbach, M.A., Wiberg, P.L., Pace, M.L., 2021. Predicting benthic macroalgal abundance in shallow coastal lagoons from geomorphology and hydrologic flow patterns. *Limnology and Oceanography* 66, 123–140.
- Blanchet, H., Gouillieux, B., Alizier, S., others, 2014. Multiscale patterns in the diversity and organization of benthic intertidal fauna among french atlantic estuaries. *Journal of Sea Research* 90, 95–110. <https://doi.org/10.1016/j.seares.2014.02.014>
- Brunier, G., Tamura, T., Anthony, E.J., Dussouillez, P., Gardel, A., 2022. Evolution of the french guiana coast from late pleistocene to holocene based on chenier and beach sand dating. *Regional Environmental Change* 22, 122.
- Calleja, F., Galván, C., Silió-Calzada, A., Juanes, J.A., Ondiviela, B., 2017. Long-term analysis of *zostera noltei*: A retrospective approach for understanding seagrasses' dynamics. *Marine environmental research* 130, 93–105.
- Castaing, P., Guilcher, A., 1995. Morphosedimentary evolution of ria-type estuaries. *Earth Surface Processes and Landforms* 20, 361–376. <https://doi.org/10.1002/esp.3290200408>
- Chadwick, K.D., Brodrick, P.G., Grant, K., Goulden, T., Henderson, A., Falco, N., Wainwright, H., Williams, K.H., Bill, M., Breckheimer, I., others, 2020. Integrating airborne remote sensing and field campaigns for ecology and earth system science. *Methods in Ecology and Evolution* 11, 1492–1508.

- Chand, S., Bolland, B., 2021. Low altitude spatial assessment and monitoring of intertidal seagrass meadows beyond the visible spectrum using a remotely piloted aircraft system. *Estuarine, Coastal and Shelf Science* 255, 107299.
- Chang, W., Cheng, J., Allaire, J., Sievert, C., Schloerke, B., Xie, Y., Allen, J., McPherson, J., Dipert, A., Borges, B., 2024. [Shiny: Web application framework for r](#).
- Cheng, G., Han, J., Lu, X., 2017. Remote sensing image scene classification: Benchmark and state of the art. *Proceedings of the IEEE* 105, 1865–1883.
- Davies, B.F.R., Gernez, P., Geraud, A., Oiry, S., Rosa, P., Zoffoli, M.L., Barillé, L., 2023. Multi-and hyperspectral classification of soft-bottom intertidal vegetation using a spectral library for coastal biodiversity remote sensing. *Remote Sensing of Environment* 290, 113554.
- Davies, B.F.R., Oiry, S., Rosa, P., Zoffoli, M.L., Sousa, A.I., Thomas, O.R., Smale, D.A., Austen, M.C., Biermann, L., Attrill, M.J., others, 2024b. A sentinel watching over intertidal seagrass phenology across western europe and north africa. *Communications Earth & Environment* 5, 382.
- Davies, B.F.R., Oiry, S., Rosa, P., Zoffoli, M.L., Sousa, A.I., Thomas, O.R., Smale, D.A., Austen, M.C., Biermann, L., Attrill, M.J., others, 2024a. Intertidal seagrass extent from sentinel-2 time-series show distinct trajectories in western europe. *Remote Sensing of Environment* 312, 114340.
- Davoult, D., Surget, G., Stiger-Pouvreau, V., Noisette, F., Riera, P., Stagnol, D., Androuin, T., Poupart, N., 2017. Multiple effects of a *gracilaria vermiculophylla* invasion on estuarine mudflat functioning and diversity. *Marine Environmental Research* 131, 227–235.
- Diruit, W., Le Bris, A., Bajjouk, T., Richier, S., Helias, M., Burel, T., Lennon, M., Guyot, A., Ar Gall, E., 2022. Seaweed habitats on the shore: Characterization through hyperspectral UAV imagery and field sampling. *Remote Sensing* 14. <https://doi.org/10.3390/rs14133124>
- Douay, F., Verpoorter, C., Duong, G., Spilmont, N., Gevaert, F., 2022. New hyperspectral procedure to discriminate intertidal macroalgae. *Remote Sensing* 14. <https://doi.org/10.3390/rs14020346>
- Douglas, T.J., Coops, N.C., Drever, M.C., Hunt, B.P., Martin, T.G., 2024. Linking microphytobenthos distribution and mudflat geomorphology under varying sedimentary regimes using unoccupied aerial vehicle (UAV)-acquired multispectral reflectance and photogrammetry. *Science of The Total Environment* 173675.
- Duffy, J.P., Pratt, L., Anderson, K., Land, P.E., Shutler, J.D., 2018. Spatial assessment of intertidal seagrass meadows using optical imaging systems and a lightweight drone. *Estuarine, Coastal and Shelf Science* 200, 169–180.
- Firth, L.B., Foggo, A., Watts, T., Knights, A.M., DeAmicis, S., 2024. Invasive macroalgae in native seagrass beds: Vectors of spread and impacts. *Annals of Botany* 133, 41–50.
- Fourcade, Y., Engler, J.O., Rödder, D., Secondi, J., 2014. Mapping species distributions with MAXENT using a geographically biased sample of presence data: A performance assessment of methods for correcting sampling bias. *PloS one* 9, e97122.
- Ginneken, V. van, Vries, E. de, others, 2018. The global dispersal of the non-endemic invasive red alga *gracilaria vermiculophylla* in the ecosystems of the euro-asia coastal waters including the wadden sea unesco world heritage coastal area: Awful or awesome? *Oceanography*

- & Fisheries Open Access Journal 8, 4–26.
- Godoy, O., Castro-Díez, P., Valladares, F., Costa-Tenorio, M., 2009. Different flowering phenology of alien invasive species in spain: Evidence for the use of an empty temporal niche? Plant Biology 11, 803–811.
- Grizel, H., Heral, M., 1991. Introduction into france of the japanese oyster (*crassostrea gigas*). ICES Journal of Marine Science 47, 399–403.
- Gurgel, C.F.D., Norris, J.N., Schmidt, W.E., Le, H.N., Fredericq, S., 2018. Systematics of the gracilariales (rhodophyta) including new subfamilies, tribes, subgenera, and two new genera, agarophyton gen. Nov. And crassa gen. nov. Phytotaxa 374, 1–23.
- Hijmans, R.J., 2024. [Terra: Spatial data analysis](#).
- IGN, 2024. Remonter le temps.
- Kazakeviciute-Januskeviciene, G., Janusonis, E., Bausys, R., Limba, T., Kiskis, M., 2020. Assessment of the segmentation of RGB remote sensing images: A subjective approach. Remote Sensing 12, 4152.
- Krueger-Hadfield, S.A., Kollars, N.M., Strand, A.E., Byers, J.E., Shainker, S.J., Terada, R., Greig, T.W., Hammann, M., Murray, D.C., Weinberger, F., others, 2017. Genetic identification of source and likely vector of a widespread marine invader. Ecology and evolution 7, 4432–4447.
- Massé, C., Viard, F., Humbert, S., Antajan, E., Auby, I., Bachelet, G., Bernard, G., Bouchet, V.M.P., Burel, T., Dauvin, J.-C., Delegrange, A., Derrien-Courtel, S., Droual, G., Gouillieux, B., Goulletquer, P., Guérin, L., Janson, A.-L., Jourde, J., Labrune, C., Lavesque, N., Leclerc, J.-C., Le Duff, M., Le Garrec, V., Noël, P., Nowaczyk, A., Pergent-Martini, C., Pezy, J.-P., Raoux, A., Raybaud, V., Ruitton, S., Sauriau, P.-G., Spilmont, N., Thibault, D., Vincent, D., Curd, A., 2023. An overview of marine non-indigenous species found in three contrasting biogeographic metropolitan french regions: Insights on distribution, origins and pathways of introduction. Diversity 15. <https://doi.org/10.3390/d15020161>
- Mcilwaine, B., Casado, M.R., Leinster, P., 2019. Using 1st derivative reflectance signatures within a remote sensing framework to identify macroalgae in marine environments. Remote Sensing 11. <https://doi.org/10.3390/rs11060704>
- Mendoza-Segura, C., Fernández, E., Beca-Carretero, P., 2023. Predicted changes in the biogeographical range of *gracilaria vermiculophylla* under present and future climate scenarios. Journal of Marine Science and Engineering 11. <https://doi.org/10.3390/jmse11020367>
- Michel, G., Le Bot, S., Lesourd, S., Lafite, R., 2021. Morpho-sedimentological and dynamic patterns in a ria type estuary: The belon estuary (south brittany, france). Journal of Maps 17, 389–400. <https://doi.org/10.1080/17445647.2021.1925170>
- Nebel, S., Beege, M., Schneider, S., Rey, G.D., 2020. A review of photogrammetry and photorealistic 3D models in education from a psychological perspective, in: Frontiers in Education. Frontiers Media SA, p. 144.
- Nurdin, N., Alevizos, E., Syamsuddin, R., Asis, H., Zainuddin, E.N., Aris, A., Oiry, S., Brunier, G., Komatsu, T., Barillé, L., 2023. Precision aquaculture drone mapping of the spatial distribution of *kappaphycus alvarezii* biomass and carrageenan. Remote Sensing 15. <https://doi.org/10.3390/rs15143674>
- Nyberg, C.D., 2007. Introduced marine macroalgae and habitat modifiers: Their ecological

- role and significant attributes. Department of Marine Ecology.
- Nyberg, C.D., Thomsen, M.S., Wallentinus, I., 2009. Flora and fauna associated with the introduced red alga *gracilaria vermiculophylla*. European Journal of Phycology 44, 395–403.
- OHMI, H., 1956. CONTRIBUTIONS TO THE KNOWLEDGE OF GRACILARIACEAE FROM JAPAN: . On a new species of the genus *gracilariopsis*, with some considerations on its ecology. 6, 271–279.
- Oiry, S., Davies, B.F.R., Pierre, G., Laurent, B., 2024a. DISCOV: Drone Intertidal Sediment Classification Of Vegetation. <https://doi.org/10.5281/zenodo.14218984>
- Oiry, S., Davies, B.F.R., Sousa, A.I., Rosa, P., Zoffoli, M.L., Brunier, G., Gernez, P., Barillé, L., 2024b. Discriminating seagrasses from green macroalgae in european intertidal areas using high-resolution multispectral drone imagery. Remote Sensing 16. <https://doi.org/10.3390/rs16234383>
- Olmedo-Masat, O.M., Raffo, M.P., Rodríguez-Pérez, D., Arijón, M., Sánchez-Carnero, N., 2020. How far can we classify macroalgae remotely? An example using a new spectral library of species from the south west atlantic (argentine patagonia). Remote Sensing 12, 3870.
- Ortega, T., Ponce, R., Forja, J., Gómez-Parra, A., 2005. Fluxes of dissolved inorganic carbon in three estuarine systems of the cantabrian sea (north of spain). Journal of Marine Systems 53, 125–142.
- Papenfuss, G.F., 1967. Notes on algal nomenclature - v. Various chlorophyceae and rhodophyceae. Phykos 5, 95–105.
- Peidro-Devesa, M.J., Martínez-Movilla, A., Rodríguez-Somoza, J.L., Sánchez, J.M., Román, M., 2024. Quantifying intertidal macroalgae stocks in the NW iberian peninsula using unmanned aerial vehicle (UAV) multispectral imagery. Regional Studies in Marine Science 103621.
- Ramus, A.P., Silliman, B.R., Thomsen, M.S., Long, Z.T., 2017. An invasive foundation species enhances multifunctionality in a coastal ecosystem. Proceedings of the national academy of sciences 114, 8580–8585.
- Roca, M., Dunbar, M.B., Román, A., Caballero, I., Zoffoli, M.L., Gernez, P., Navarro, G., 2022. Monitoring the marine invasive alien species *rugulopteryx okamurae* using unmanned aerial vehicles and satellites. Frontiers in Marine Science 9, 1004012.
- Román, A., Oiry, S., Davies, B.F., Rosa, P., Gernez, P., Tovar-Sánchez, A., Navarro, G., Méléder, V., Barillé, L., 2024. Mapping intertidal microphytobenthic biomass with very high-resolution remote sensing imagery in an estuarine system. Science of The Total Environment 177025.
- Román, A., Tovar-Sánchez, A., Olivé, I., Navarro, G., 2021. Using a UAV-mounted multispectral camera for the monitoring of marine macrophytes. Frontiers in Marine Science 8, 722698.
- Romero, M., Andrés, A., Alonso, R., Viguri, J., Rincón, J.M., 2008. Sintering behaviour of ceramic bodies from contaminated marine sediments. Ceramics International 34, 1917–1924.
- Rueness, J., 2005. Life history and molecular sequences of *gracilaria vermiculophylla* (gracilar-

- iales, rhodophyta), a new introduction to european waters. *Phycologia* 44, 120–128.
- Savitzky, A., Golay, M.J., 1964. Smoothing and differentiation of data by simplified least squares procedures. *Analytical chemistry* 36, 1627–1639.
- Sfriso, A., Wolf, M.A., Maistro, S., Sciuto, K., Moro, I., 2012. Spreading and autoecology of the invasive species *gracilaria vermiculophylla* (gracilariales, rhodophyta) in the lagoons of the north-western adriatic sea (mediterranean sea, italy). *Estuarine, Coastal and Shelf Science* 114, 192–198.
- Simon, O., 2024. [Shiny app for validation dataset building](#).
- Sotka, E.E., Baumgardner, A.W., Bippus, P.M., Destombe, C., Duermit, E.A., Endo, H., Flanagan, B.A., Kamiya, M., Lees, L.E., Murren, C.J., others, 2018. Combining niche shift and population genetic analyses predicts rapid phenotypic evolution during invasion. *Evolutionary Applications* 11, 781–793.
- Surget, G., 2017. Processus adaptatifs des végétaux marins face au changement climatique à différentes échelles de temps et d'espace: Dynamique de populations, métabolomique, éco-physiologie et potentiels de valorisation (PhD thesis). Université de Bretagne occidentale-Brest.
- Tankoua, O.F., Buffet, P.-E., Amiard, J.-C., Amiard-Triquet, C., Mouneyrac, C., Berthet, B., 2011. Potential influence of confounding factors (size, salinity) on biomarkers in the sentinel species *scrobicularia plana* used in programmes monitoring estuarine quality. *Environmental Science and Pollution Research* 18, 1253–1263. <https://doi.org/10.1007/s11356-011-0479-3>
- Terada, R., Yamamoto, H., 2002. Review of *gracilaria vermiculophylla* (ohmi) papenfuss and other species in japan and asia. *Taxonomy of economic seaweeds, with special reference to Pacific species* 8, 225–230.
- Thomsen, M.S., McGlathery, K., Schwarzschild, A., Silliman, B., 2009. Distribution and ecological role of the non-native macroalga *gracilaria vermiculophylla* in virginia salt marshes. *Biological Invasions* 11, 2303–2316.
- Thomsen, M.S., Staehr, P.A., Nyberg, C.D., Schwærter, S., Krause-Jensen, D., Silliman, B.R., 2007. *Gracilaria vermiculophylla* (ohmi) papenfuss, 1967 (rhodophyta, graciliaceae) in northern europe, with emphasis on danish conditions, and what to expect in the future. *Aquatic invasions* 2, 83–94.
- Thomsen, M.S., Stæhr, P.A., Nejrup, L., Schiel, D.R., 2013. Effects of the invasive macroalgae *gracilaria vermiculophylla* on two co-occurring foundation species and associated invertebrates. *Aquatic Invasions* 8, 133–145.
- Valle, M., Pala, V., Lafon, V., Dehouck, A., Garmendia, J.M., Borja, A., Chust, G., 2015. Mapping estuarine habitats using airborne hyperspectral imagery, with special focus on seagrass meadows. *Estuarine, Coastal and Shelf Science* 164, 433–442.
- Van Katwijk, M., 2003. Reintroduction of eelgrass (*zostera marina l.*) in the dutch wadden sea: A research overview and management vision, in: Challenges to the Wadden Sea Area. In: Proceedings of the 10th International Scientific Wadden Sea Symposium, Groningen, the Netherlands. pp. 173–195.
- Vilizzi, L., Copp, G.H., Hill, J.E., Adamovich, B., Aislabie, L., Akin, D., Al-Faisal, A.J., Almeida, D., Azmai, M.A., Bakiu, R., others, 2021. A global-scale screening of non-native

- aquatic organisms to identify potentially invasive species under current and future climate conditions. *Science of the Total Environment* 788, 147868.
- Weinberger, F., Buchholz, B., Karez, R., Wahl, M., 2008. The invasive red alga *gracilaria vermiculophylla* in the baltic sea: Adaptation to brackish water may compensate for light limitation. *Aquatic Biology* 3, 251–264.
- Williams, S.L., Smith, J.E., 2007. A global review of the distribution, taxonomy, and impacts of introduced seaweeds. *Annu. Rev. Ecol. Evol. Syst.* 38, 327–359.
- Zenetas, A., Tsiamis, K., Galanidi, M., Carvalho, N., Bartilotti, C., Canning-Clode, J., Castriota, L., Chainho, P., Comas-González, R., Costa, A.C., Dragičević, B., Dulčić, J., Faasse, M., Florin, A.-B., Gittenberger, A., Jakobsen, H., Jelmert, A., Kerckhof, F., Lehtiniemi, M., Livi, S., Lundgreen, K., Macic, V., Massé, C., Mavrič, B., Naddafi, R., Orlando-Bonaca, M., Petovic, S., Png-Gonzalez, L., Carbonell Quetglas, A., Ribeiro, R.S., Cidade, T., Smolders, S., Stæhr, P.A.U., Viard, F., Outinen, O., 2022. Status and trends in the rate of introduction of marine non-indigenous species in european seas. *Diversity* 14. <https://doi.org/10.3390/d14121077>
- Zoffoli, M.L., Gernez, P., Godet, L., Peters, S., Oiry, S., Barillé, L., 2021. Decadal increase in the ecological status of a north-atlantic intertidal seagrass meadow observed with multi-mission satellite time-series. *Ecological Indicators* 130, 108033.
- Zoffoli, M.L., Gernez, P., Oiry, S., Godet, L., Dalloyau, S., Davies, B.F.R., Barillé, L., 2023. Remote sensing in seagrass ecology: Coupled dynamics between migratory herbivorous birds and intertidal meadows observed by satellite during four decades. *Remote Sensing in Ecology and Conservation* 9, 420–433.